



Article

Sand Supply Affects Wind Erosion Efficiency and Sand Transport on Sand-Cemented Body Mulch Bed

Jie Zhou¹, Haifeng Wang¹ and Beibei Han^{2,*}

¹ National Engineering Technology Research Center for Desert-Oasis Ecological Construction, Xinjiang Institute of Ecology and Geography, Chinese Academy of Sciences, Urumqi 830011, China; zhoujie@ms.xjb.ac.cn (J.Z.); wanghf@ms.xjb.ac.cn (H.W.)

² College of Resources and Environment, Xinjiang Agricultural University, Urumqi 830052, China

* Correspondence: beibehan@xjau.edu.cn

Abstract: Sand-cemented bodies (SCBs) are naturally distributed in some interdune corridors in the central Taklimakan Desert, northwest China. In this study, field-collected SCB particles were used as the experimental material, and wind tunnel experiments were conducted with different sand supplies, wind velocities, and SCB coverages to evaluate SCB wind erosion efficiency and vertical mass flux. The results showed that wind erosion efficiency decreased as SCB coverage increased. When the SCB coverage was above 40%, sand deposition processes occurred only under saturated sand flow, while sand transport remained unaffected by increases in SCB coverage under unsaturated sand flow. Under saturated flow, the highest concentrations of transported sand were found at 0–6 cm above the surface, and the main sand bed process was deposition. The sand bed process changed from aeolian erosion to deposition with increasing SCB coverage and tended to remain stable until the SCB coverage exceeded 40%. By contrast, under unsaturated sand flow, the sand bed process was primarily aeolian erosion, and the highest concentrations of transported sand were found at 0–4 cm above the surface. At high SCB coverage levels (more than 40%), a general balance between aeolian erosion and deposition processes was reached. In summary, increasing SCB coverage had a significant impact on surface wind erosion processes. Thus, SCBs can be used as a novel sand retention material.



Citation: Zhou, J.; Wang, H.; Han, B. Sand Supply Affects Wind Erosion Efficiency and Sand Transport on Sand-Cemented Body Mulch Bed. *Atmosphere* **2024**, *15*, 571. <https://doi.org/10.3390/atmos15050571>

Academic Editor: Thomas Gill

Received: 15 March 2024

Revised: 30 April 2024

Accepted: 4 May 2024

Published: 7 May 2024



Copyright: © 2024 by the authors. Licensee MDPI, Basel, Switzerland. This article is an open access article distributed under the terms and conditions of the Creative Commons Attribution (CC BY) license (<https://creativecommons.org/licenses/by/4.0/>).

1. Introduction

Wind erosion is a major cause of environmental hazards in arid and semi-arid regions. The Taklamakan Desert is located deep within Asia and is characterized by its aridity, frequent sandstorms, fine-grained surface materials, and significant wind erosion hazards. Wind erosion, resulting in the detachment, transportation, and redeposition of soil particles, degrades soil productivity through removing the fertile topsoil, leading to serious farmland deterioration [1,2]. Aeolian erosion, transportation, and deposition are the basic processes on wind-blown sand beds, and these processes directly represent the differentiation of wind-sand flow structures. The underlying surface conditions are the most important factor that influences the erosion–deposition status of the bed, causing different variations in wind-sand flow structures [3,4].

Various conservation measures have been used in both the laboratory and field to combat wind erosion [5,6]. The control methods include mechanical, chemical, and biological approaches. Mechanical control measures include the construction of barriers, such as straw checkerboard barriers and sand fences, to prevent the movement of sand [7]. Chemical control involves forming a crust on the soil surface with various chemicals, such as bitumen or latex [8]. Biological control measures involve planting vegetation as windbreaks [9,10].

Mechanical and biological controls such as barriers, sand fences, and windbreaks can improve the wind speed threshold for soil loss through absorbing the partial wind momentum and decreasing the aerodynamic forces on the erodible particles [11]. However, due to their limited capacity to fix sand and the need for regular maintenance, these methods can be used on desert roads and in gas/oil fields only as a temporary and auxiliary means of sand control. Chemical control measures should only be used to fix the sand issue, not the flow issue. In addition, the issue of secondary environmental pollution must be considered [6]. Implementation of the aforementioned measures presents several challenges in preventing wind erosion.

The underlying surface conditions are the most important factor influencing the erosion–deposition status of the bed, which also cause variations in wind-sand flow structures [12]. In recent decades, many scholars have conducted research on the feedback mechanism of the variations in aeolian erosion–deposition and blowing-sand structures on gravel beds. This research has focused on both wind tunnel simulations and field observations [13–16]. Zhang et al. [17] reported that an exponential decrease in wind erosion on an erodible bed could be achieved in wind tunnel simulations through increasing the gravel cover. Tan et al. [18], comparing the same surface without the tested gravels, showed that gravel beds can obviously reduce sand transport, and increasing the gravel size also helped to reduce it. The utilization of gravel mulch not only reduces surface wind erosion intensity but can also effectively minimize the release of surface sand and dust. When placed on sand, gravel mulch is non-erodible and enhances surface roughness, increasing surface resistance. Therefore, gravel helps to protect topsoil from wind erosion, similar to straw checkerboard barriers or sand fences [15,16]. In addition, gravel mulch has been widely used in various applications, such as sand fixation, roadside erosion protection, and slope stabilization, due to its low cost and easy availability compared to chemical control measures.

Aeolian erosion, transportation, and deposition are the basic processes of wind-blown sand beds and can directly represent the differentiation of wind-sand flow structures. In recent decades, there have been more studies on the mutual feedback mechanism between bed erosion and sand flow. However, the structural changes in sand flow and bed erosion caused by the sand supply degree and wind speed have not been thoroughly investigated [18–20]. The sand supply abundance determines the saturation degree of the wind-sand flow and the erosion it causes on gravel beds. Hence, the sand supply plays an important role in the various bed processes that form with the wind-sand flow. The sediment input from the bed is one of the important indices used to judge whether sand bed processes are primarily associated with erosion or deposition [21–23]. Zhang et al. [23] pointed out that the environmental conditions in the aeolian region, especially the surface material composition and sand source abundance, have significant impacts on near-surface sand transport and wind-sand flow structures. According to Wilcock et al. [21], the total transport rate and gravel transport rate are highly dependent on the sand content. Zhang et al. [24] reported that the use of mechanical sand barriers in different sand supply environments further affects bed processes in the area where mechanical sand barriers are deployed.

Sand-cemented bodies (SCBs) are naturally dispersed in multiple interdune corridors of the central Taklimakan Desert in northwestern China. SCBs consist of diverse sand particle sizes and possess a firm texture resembling gravel, and their average specific gravity ($2.486\text{--}2.534 \text{ g cm}^{-3}$) is equal to that of natural gravel ($2.652\text{--}2.751 \text{ g cm}^{-3}$). SCBs are very irregular, difficult to separate, and scattered in the interdune corridors of the region, which has resulted in a large granular layer of coarse sand lying on top of the sand surface, similar to gravel mulch beds (see Figure 1).

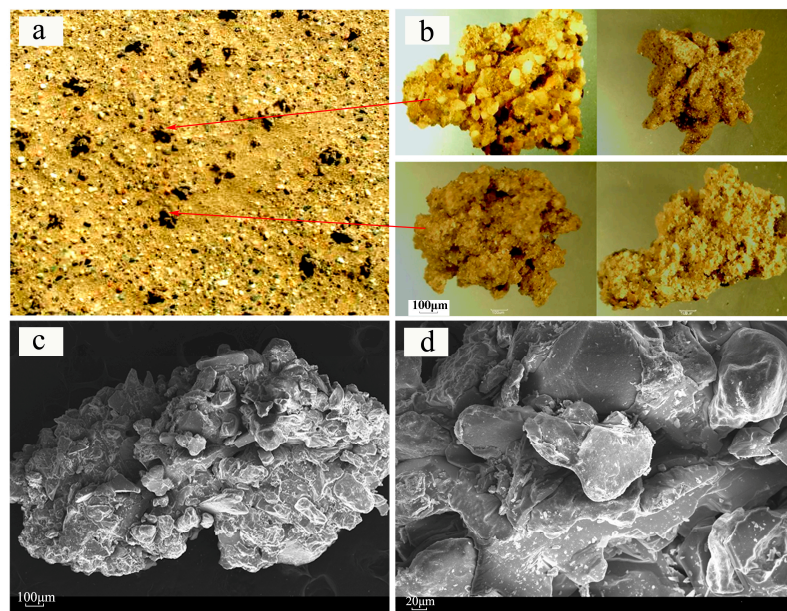


Figure 1. SCBs from the sandy surface in the central Taklamakan Desert region: (a) close view of the SCBs marked by red arrows; (b) SCB shapes under stereo-microscope (magnification: $\times 50$); (c) SCB micro-morphology (magnification: $\times 50$); (d) SCB micro-morphology (magnification: $\times 100$).

Wind-blown sand occurs frequently and damages agricultural infrastructures, desert traffic trunks, and gas and oil fields. Therefore, effective and scientific control over wind erosion in arid desert regions has become a new challenge in the northwest of China. Previous studies have documented that gravel mulch can be used to combat wind erosion [12,25–28]. Given the similarity between SCBs and gravel and the lack of research on SCBs, it is necessary to consider their application as a natural wind-resistant material in sandy areas. The objects of this study were as follows: (1) to evaluate the erosion efficiency effect under different SCB coverages and sand supplies; and (2) to reveal the influence of the sand supply on sand transport and wind-sand flow structure under different SCB coverages. The results of this study provide further information on the use of SCBs in aeolian geomorphology and blown-sand control engineering. In addition, this study may provide a theoretical basis for the exploitation and application of SCBs as a natural sand-fixing material.

2. Materials and Methods

2.1. Materials

For this study, sandy soil was collected from the shifting dune surface of the Taklimakan Desert in the center of the Tarim Basin, Xinjiang Uygur Autonomous Region, China ($39^{\circ}05'99''$ N, $83^{\circ}64'04''$ E). Particle size (Figure 2) analysis was performed using a laser particle size analyzer (Malvern MS-2000, Brighton, Britain). The chemical composition of soluble matter of SCBs collected from interdune corridors in the central Taklimakan Desert ($39^{\circ}04'90''$ N, $83^{\circ}64'14''$ E) is shown in Table 1.

Table 1. Chemical composition of the soluble matter of SCBs.

Mineral Composition (%)						Average Conductivity ($\text{m}\cdot\text{Scm}^{-1}$)	Average pH
CaSO_4	NaCl	CaCl_2	MgCl_2	KCl	$\text{Mg}(\text{HCO}_3)_2$		
79.67	6.87	6.20	5.62	1.22	0.42	2.57	7.40

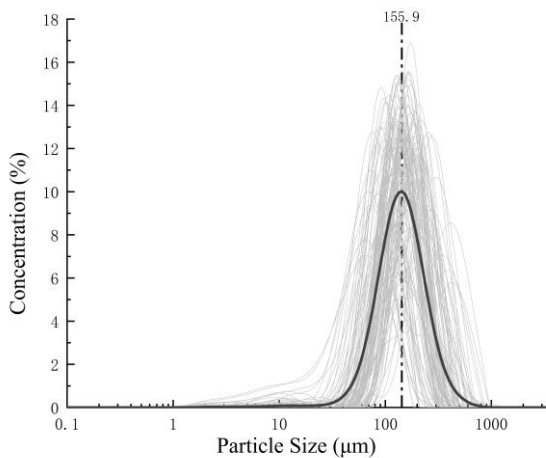


Figure 2. Distribution of sand particle size, black line is the average (sand samples consisted primarily of fine sand and very fine sand).

2.2. Experimental Design

Wind tunnel simulations were conducted at the Environmental Wind Tunnel Laboratory (direct current blowing wind tunnel) of the Xinjiang Institute of Ecology and Geography, Chinese Academy of Sciences. The wind tunnel was 16 m in length, with an 8 m experimental section (cross section: 1×1.3 m). The wind velocity was controlled continuously ($0\text{--}25\text{ ms}^{-1}$), and the boundary layer thickness could be set to 15–25 cm [22].

Sand tables with different SCB coverages were prepared (0% = CK, 2%, 5%, 8%, 10%, 20%, 40%, and 80%). The wind velocity was measured using a hot wire anemometer in front of the experimental section at a distance of 40 cm from the side wall (Figure 3). Wind speeds of 8 ms^{-1} (10 min), 10 ms^{-1} (5 min), and 15 ms^{-1} (3 min) were replicated three times for each treatment combination under different sand supplies (saturated and unsaturated sand flows). The saturated sand flow was a 5 cm thick bed of sand placed in the center of the test section with a cross section of a 1.0 m width and 2.0 m length (Figure 3, sandy bed). The unsaturated sand flow was only pure wind.

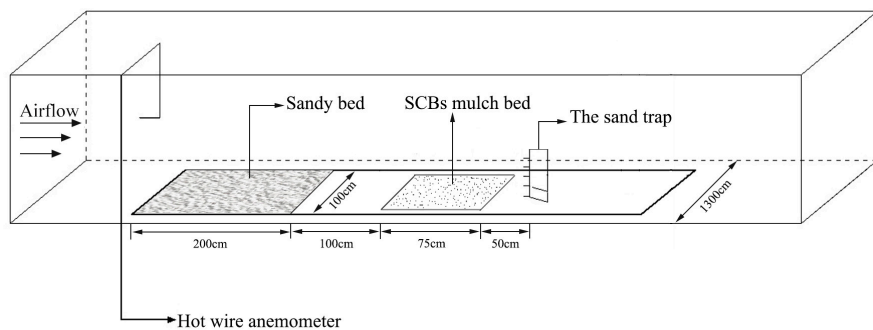


Figure 3. The experimental layout.

To quantify sand erosion efficiency, we set a sand table of 75×50 cm in the center of the experimental section. In addition, to determine the blowing-sand flux variation with height, a vertical sand trap was used to measure the sand transport at various heights along the lee side of the sand tray. The vertical sand trap was divided into openings of 1×1 cm to collect the blowing sand at 20 levels. The vertical sand trap was wind-tunnel-verified and captured over 90% of the moving sand.

2.3. Wind Erosion Efficiency

Wind erosion efficiency (R) ($\text{kg cm}^{-2} \text{ min}^{-1}$) was calculated by measuring the amount of sand (kg) transported by the wind from a certain area (cm^2) and at a certain time (min), determined as follows:

$$R = (W_a - W_b)/(S \times T) \quad (1)$$

where W_a and W_b are the overall masses (kg) of the sand tables. Prior to and after blowing, S is the sand table area (cm^2) and T is the blowing duration (min). A W_b greater than W_a indicates that the SCB mulch bed process is deposition, and a W_a greater than W_b indicates that the SCB mulch bed process is erosion.

2.4. Sand Flux Profile

The sand flux profile was used to measure the amount of sand transported in a specified airflow layer, calculated as the amount of transported sand per unit of width perpendicular to the blow direction and per unit of time:

$$q_z = q_0 \exp(-kz) \quad (2)$$

where q_z is the mass sand transport at vertical height (z) (cm), and q_0 is the creep mass ($\text{g cm}^{-2} \text{s}^{-1}$) sand transport at the surface ($z = 0$), where k is the decay factor.

3. Results and Discussion

3.1. Wind Erosion Efficiency Variation with Different Sand Supplies and SCB Coverages

Under saturated sand flow conditions, wind erosion efficiency was highly sensitive to SCB coverage but had little effect on wind speed at the sand surface, as illustrated in Figure 4a, which was mainly due to increases in SCB coverage and sand supply, which increased the particle collision kinetic energy, resulting in enhanced sand transport. Nickling and Neuman [29] noted that wind–bed interaction intensity is the main cause of elastic collisions between bed roughness elements and sand particles, and an increase in elastic collisions directly leads to an increase in sand transport rate.

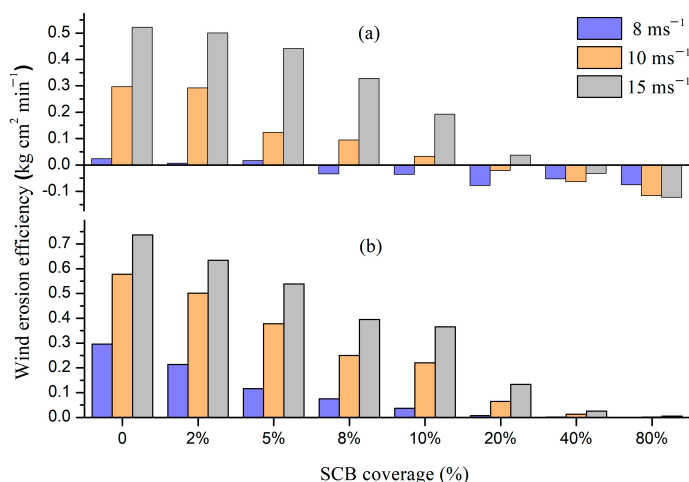


Figure 4. Wind erosion efficiency with different SCB coverages and wind velocities: (a) saturated sand flow; (b) unsaturated sand flow (positive values indicate that the SCB mulch bed process was deposition, and negative values indicate that the SCB mulch bed process was erosion).

Under saturated sand flow, the higher the wind speed, the less effective the wind erosion, and the sand surface process shifted from erosion to accumulation. At an SCB coverage of 8% under 8 ms^{-1} , the bed surface started to produce wind accumulation (the wind erosion was $-0.033 \text{ kg cm}^{-2} \text{ min}^{-1}$, indicating that the SCB mulch bed process was deposition), and when the SCB coverage was 20–80% of the bed, the sand had essentially

been deposited. Li et al. [30] revealed that gravel trapping has an important effect on the amount of sand available for transport.

Sand deposition occurs in areas of reduced shear behind gravel. As the gravel coverage increases (the space shrinks), the shear stress distribution causes sand deposition in the spaces between gravel particles, further reducing the amount of sand available for transport. This explains the sand particle deposition on the bed under saturated wind flow, while under unsaturated flow, the bed surface stabilized with over 40% SCB coverage, resulting in a wind erosion efficiency below $0.0018 \text{ kg cm}^{-2} \text{ min}^{-1}$ at any velocity. The SCBs in the mulch bed prevented wind erosion and accumulation (Figure 4b). Li et al. [30] and Al-Awadhi and Willetts [31] demonstrated that sand transport remained unchanged when the gravel coverage reached 50% or more.

Cai et al. [22] demonstrated that sand supply abundance can significantly reduce the wind erosion rate so that under saturated wind-sand flow conditions, the sand bed surface shows a stable sand accumulation state. The bed process was mainly deposition when controlled by saturated sand flow (Figure 5a). The accumulated amount of sand increased with increasing wind velocity and decreased with increasing SCB coverage. When the wind velocity was 8 ms^{-1} , the bed process was slight aeolian erosion at 0 and 5% SCB coverage, and it was deposition at the other coverage levels. When the wind velocity was 15 ms^{-1} , the deposition process occurred only within the SCB coverage range of 40–80%, while aeolian erosion dominated in the other SCB coverage ranges. The accumulated sand amount decreased with the increase in SCB coverage. When the SCB coverage exceeded 40%, the bed process was complete deposition at all wind velocities. When the SCB coverage was from 8% to 20%, the bed process was deposition at low wind velocities and changed to aeolian erosion as the wind velocity increased.

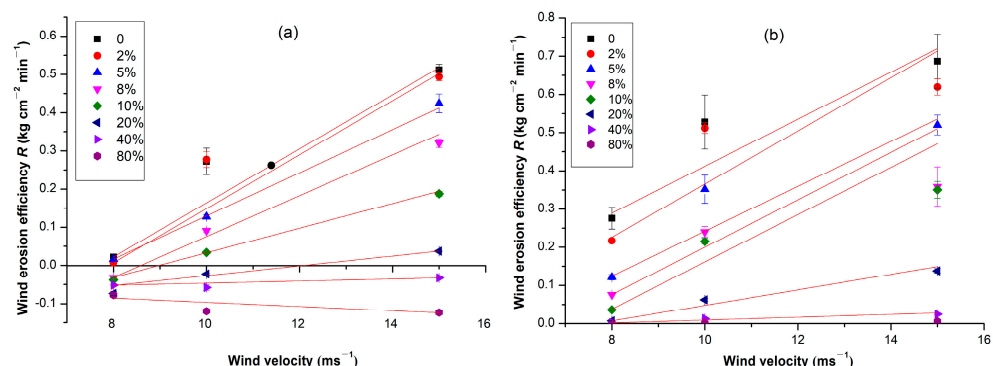


Figure 5. Wind erosion efficiency with wind velocities at different SCB coverage levels: (a) under saturated sand flow, the bed process was full deposition with higher coverage; (b) under unsaturated sand flow, the bed process was complete erosion.

At SCB coverages below 8%, the sand accumulation due to wind speed was significant (see Table 2; mean slope (b): 0.50). Therefore, the wind velocity caused significant changes in sand transport. When the SCB coverage level was between 10% and 20%, the curve slope became lower (slope (b), change from 0.32 to 0.15; Table 2). Correspondingly, surface SCB coverage began to play an important role in sand transportation. The increasing wind velocity caused the proportion of transportable and wind-blown sand to increase, and the transportation process was controlled by saturated flow. When the SCB coverage was above 40%, sand accumulation decreased as wind speed increased, as shown in Table 2 (slope (b): 0.036). The varying accumulated sand amounts at higher SCB coverage showed that sand accumulation and transportation can be managed effectively if the SCB coverage is maintained above 40%. Earlier studies reported that an equilibrated surface should have a gravel coverage from 40% to 80% [32–35], and our results supported this conclusion.

Table 2. Linear regression ($y = a + bx$) between wind velocity and accumulated sand amount at varying SCB coverage levels under saturated sand flow.

SCB Coverage (%)	a (Intercept)	b (Slope)
0	−0.447	0.662
2	−0.449	0.650
5	−0.534	0.652
8	−0.428	0.507
10	−0.293	0.324
20	−0.191	0.155
40	−0.089	0.036
80	−0.041	0.058

As shown in Figure 5b, the bed processes consisted entirely of erosion and transport when controlled by unsaturated sand flow. Evidence of aeolian erosion was present in all beds, and the amount of wind-eroded sand increased with increasing wind speed. At lower SCB coverage levels, the increase in accumulated sand amount with wind velocity was greater. The results indicated that the accumulated sand amount was more affected by wind speed at low SCB coverage levels. To illustrate this further, Figure 5b presents the curve slopes indicating the correlation between sand accumulation amount and wind speed under different SCB coverages. When the SCB coverage was below 10%, there was a significant increase in the accumulated sand amount as the wind velocity increased (mean slope, $b = 0.55$; Table 3).

Table 3. Linear regression ($y = a + bx$) between wind velocity and accumulated sand amount at varying SCB coverage levels under unsaturated sand flow.

SCB Coverage (%)	a (Intercept)	b (Slope)
0	2.596	0.397
2	0.435	0.508
5	−1.460	0.547
8	−3.285	0.629
10	−4.184	0.683
20	−1.933	0.278
40	−0.281	0.032
80	−0.086	0.011

Thus, in this situation, intense changes in sand transport were likely to occur due to variations in wind velocity, illustrating that sand transport was influenced by wind speed even at low SCB coverage levels. However, when the SCB coverage reached 20%, the curve slope began to decrease ($b = 0.28$; Table 3), indicating that the amount of sand collected was affected by SCB coverage on the sand bed.

Higher SCB coverage resulted in increased surface roughness and drag, which likely improved the erosion resistance of the sand by reducing the airflow momentum. In this study, the sand accumulation amount due to wind speed was not significant. With an SCB coverage above 40%, the accumulated sand amount changed slightly with wind speed (very small mean slope, $b = 0.03$; Table 3). The change in the accumulated amount of sand was stable with high SCB coverage and reached a general balance between aeolian erosion and deposition.

Dong et al. [14] concluded that the maximum aerodynamic roughness length occurred between 40% and 75% gravel coverage, indicating that even partially gravel-covered, wind-eroded sand surfaces may become stable. This helps to explain why the accumulated sand amount decreased minimally as the SCB coverage exceeded 40%.

3.2. Horizontal Mass Flux Vertical Profiles at Different SCB Coverages and Sand Supplies

The sand transport rate reflects the amount of sand transported, which is influenced by wind velocity and sand supply. Based on the results from the wind tunnel experiments of the horizontal mass flux vertical profile being controlled by saturated sand flow, all of the mass flux profiles exhibited almost exponential decreases in q_z (Equation (2)) with height (see Figure 6), similar to the findings of Zheng et al. [36], who found that the mass flux at the sand surface exponentially decreased with height.

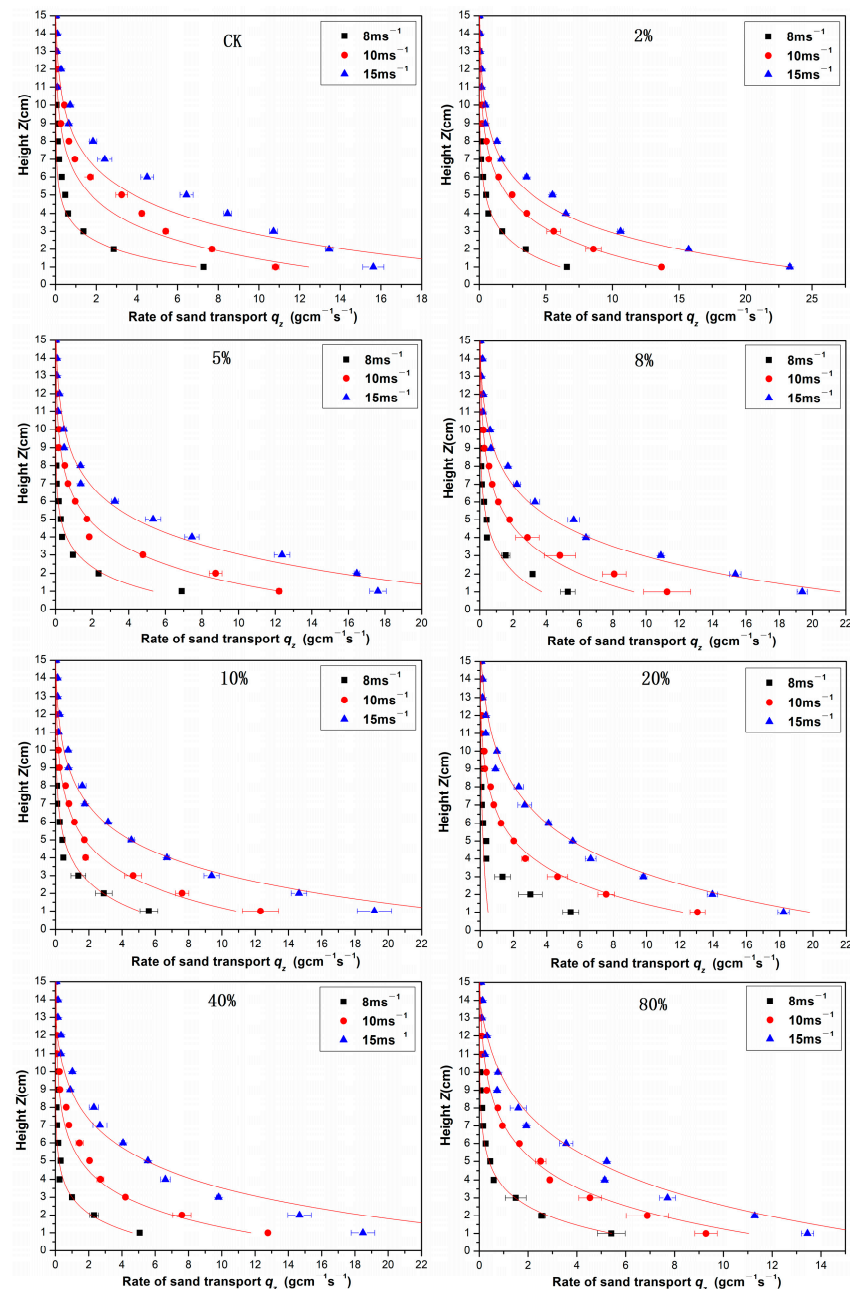


Figure 6. Height variation (Z) of horizontal sediment mass flux changes with various SCB coverages and wind speeds under saturated sand flow. The red curves are the sand transport decay curves on the SCB mulch sand bed (Equation (2)).

At a low wind velocity (8 ms^{-1}), the sand particles mostly crept along the surface, with few saltated to higher layers. As the wind velocity increased, the saltating sands increased further. For instance, when the wind velocity was 8 ms^{-1} , the saltation height only reached

6 cm, while at the 15 ms^{-1} wind velocity, a small part of the sand saltation reached 10 cm or higher, indicating that at heights of 0–6 cm, the horizontal mass flux vertical profile varied with increasing wind speed.

In addition, the sand transport rate became higher with increasing wind speed. For example, when the SCB coverage was 2%, the sand transport rates were 6.46, 13.58, and $23.34 \text{ cm}^{-1}\text{min}^{-1}$ at 8, 10, and 15 ms^{-1} , respectively, indicating that the horizontal mass flux vertical profile was well-developed with increasing wind velocity. As the SCB coverage ranged from 0 to 10%, the sand transport near the surface increased with increasing SCB coverage and reached the maximum value of $23.34 \text{ g cm}^{-1}\text{min}^{-1}$ at 2% SCB coverage. This increase was mainly due to the increase in strong elastic collisions between the saltating sands and SCBs, which eventually transferred some of the momentum to the intervening sand beds. As the coverage reached 20%, the horizontal mass flux vertical profile near the surface had a higher curvature. For example, at 15 ms^{-1} , the near-surface sand transport rate was $17.98 \text{ g cm}^{-1}\text{min}^{-1}$ at 20% SCB coverage, which was higher than that at 0% coverage ($15.99 \text{ g cm}^{-1}\text{min}^{-1}$), indicating that the bed process began to switch to deposition at 20% SCB coverage. When the SCB coverage exceeded 40%, the sediment deposition process tended to stabilize, and there was no change in the curvature of the sand transport vertical profile.

The maximum sand transport rates at 40% and 80% SCB coverage were 14.35 and $13.62 \text{ g cm}^{-1}\text{min}^{-1}$ at 15 ms^{-1} , respectively, which were less than those of the other kinds of SCB mulch beds. This was mainly because as the SCB coverage increased, the non-erodible particles (SCBs) present on the erodible sand surface absorbed some of the wind momentum flux [37]. Li et al. [30] pointed out that the distribution of shear stress causes the deposition of sand in the spaces between the gravel, further reducing the amount of sand available for transport.

Wu et al. [38] reported that, at similar heights, the amount of sand transported in near-surface sand beds increased with the increasing amount of sand transported at different wind velocities. Similarly, in this study, the amount of sand transported near the surface sand bed (at 0–6 cm) increased significantly with increasing wind speed (Table A1).

As the wind velocity increased, more than 90% of sand transport occurred at 0–6 cm because of the fence effect of the SCBs on the surface bed. By contrast, at 6–15 cm, the transported sand amounts at different coverage levels and wind velocities were relatively small. For example, when the sand bed had 5% coverage and the wind velocity was 8 ms^{-1} , the sand transport amounts above the surface at 0–2, 2–4, 4–6, and 6–15 cm were 9.31, 1.38, 0.46, and $0.14 \text{ g cm}^{-1}\text{min}^{-1}$, respectively. However, when the wind velocity was 15 ms^{-1} , the sand transport amounts above the surface at 0–2, 2–4, 4–6, and 6–15 cm were 33.65, 19.24, 8.14, and $4.45 \text{ g cm}^{-1}\text{min}^{-1}$, respectively (3.6, 14, 17, and 31 times those at 8 ms^{-1} , respectively).

With the increase in SCB coverage, there was a decrease in aeolian erosion and deposition on the SCB beds.

However, there was no reduction in the amount of sand transported within 6 cm from the surface sand bed, even at the same wind velocity. For example, at 8 ms^{-1} , when the bed had 10% SCB coverage, the sand transport amounts at 0–2, 2–4, and 4–6 cm above the surface were 7.78, 1.42, and $0.59 \text{ g cm}^{-1}\text{min}^{-1}$, respectively. By contrast, when the bed had 80% SCB coverage, the sand transport amounts were 7.48, 1.72, and $0.69 \text{ g cm}^{-1}\text{min}^{-1}$ at 0–2, 2–4, and 4–6 cm above the surface, respectively. At 15 ms^{-1} , when the bed had 10% SCB coverage, the sand transport amounts at 0–2, 2–4, and 4–6 cm above the surface were 28.29, 16.51, and $7.86 \text{ g cm}^{-1}\text{min}^{-1}$, respectively. By contrast, the transport amounts at 0–2, 2–4, and 4–6 cm above the surface were 24.99, 13.13, and $8.99 \text{ g cm}^{-1}\text{min}^{-1}$, respectively, when the bed had 80% SCB coverage (Table A1), which was mainly due to the increasing SCB coverage protecting the surface bed through absorbing the wind momentum, thereby decreasing aeolian erosion. However, under saturated flow, the interaction increased on the SCB mulch beds. In addition, the collision between sand particles and SCBs increased, and the sand particles could take off at higher wind speeds [18].

Sand supply abundance is a key factor in identifying sand stream saturation. The sand supply abundance influenced the horizontal mass flow vertical profile and also affected the aeolian erosion and deposition properties of the SCB coverage beds [23]. As shown in Figure 7, under unsaturated flow conditions, the sand transport curve still followed an exponential function, and the SCB coverage increase resulted in decreases in the curvature of the horizontal mass flux vertical profile and sand transport rate. For example, with an SCB coverage below 10%, no significant modification in the curve occurred, and the effect of the coverage on the sand transport profile was marginal. With SCB coverages ranging from 10% to 40%, the sand transport profile decreased rapidly with height, particularly at the base of the sand cloud at low wind speed (8 ms^{-1}). With an SCB coverage above 40%, there was no sand transport at low wind speed, and the sand transport profile was only slightly reduced (8 ms^{-1}), implying that the cover mainly affected the sand transport profile near the cloud base.

Under unsaturated sand flow, saltating sands developed closer together than those under saturated sand flow, which may be due to the fact that more momentum is transferred to the intervening sand beds under saturated flows, resulting in stronger elastic collisions between saltating particles and increased surface roughness elements [29].

For the same SCB coverage, the sand transport rate increased with wind speed. The increase extent became smaller, and the main concentration of the transported sand amounts occurred at 0–4 cm above the surface (Table A2). For example, when the SCB coverage was 5%, the amounts of transported sand at 0–4 cm were 1.93, 9.39, and $17.17 \text{ g cm}^{-1}\text{min}^{-1}$ at 8, 10, and 15 ms^{-1} , respectively (95%, 88%, and 80% of the transported sand amount above the bed, respectively). As the SCB coverage reached 10%, the transported sand amounts at 0–4 cm above the surface were 0.65, 6.45, and $16.79 \text{ g cm}^{-1}\text{min}^{-1}$ at 8, 10, and 15 ms^{-1} , respectively (94%, 93%, and 86% of the transported sand amount above the bed, respectively) indicating that, as the wind velocity increased, the creeping and saltating sand amounts both increased.

In contrast to the those under saturated sand flow, the saltating sand particles reached up to 4 cm or less above the surface, as only the wind momentum was transferred to the SCB particles and saltating sand. For example, at 5% SCB coverage, the amounts of transported sand at 0–4 cm were 1.93, 9.39, and $17.17 \text{ g cm}^{-1}\text{min}^{-1}$ at 8, 10, and 15 ms^{-1} , respectively (95%, 88%, and 80% of the transported sand amount above the bed, respectively).

With the same wind speed, the sand transport rate was reduced with SCB coverage and, thus, the decreasing transported sand amount trend became less clear (Table A2). For instance, when the sand bed had 40% SCB coverage, the transported sand amounts at all heights were 0 at 8 ms^{-1} and 0.65, 0.24, 0.14, and $0.06 \text{ g cm}^{-1}\text{min}^{-1}$ at 0–2, 2–4, 4–6, and 6–10 cm above the surface, respectively. When the wind velocity was 8 ms^{-1} , the transported sand amounts at 0–2, 2–4, 4–6, and 6–10 cm above the 5% SCB coverage were 1.61, 0.32, 0.08, and $0.01 \text{ g cm}^{-1}\text{min}^{-1}$, respectively; however, they were 0.54, 0.11, 0.03, and $0 \text{ g cm}^{-1}\text{min}^{-1}$, respectively, when the SCB coverage was 10%. As the SCB coverage further increased, the aeolian erosion action over the SCB mulch beds was dramatically weakened. The horizontal mass flux vertical profile was primarily concentrated at 0–2 cm above the surface. When the sand bed had 40% SCB coverage, the transported sand amounts at all heights were 0 at 8 ms^{-1} and 0.65, 0.24, 0.14, and $0.06 \text{ g cm}^{-1}\text{min}^{-1}$ at 0–2, 2–4, 4–6, and 6–10 cm above the surface, respectively (Table A2). These results suggested that the bed's aeolian erosion process began to balance at higher SCB coverage levels (i.e., more than 40%).

Previous studies have recommended that gravel coverage from 40 to 80% provides an equilibrated surface [32–35]. Our results demonstrated that SCB mulch may provide a similar advantage to gravel mulch in controlling surface sediment movement and, thus, could be a viable sand retention material.

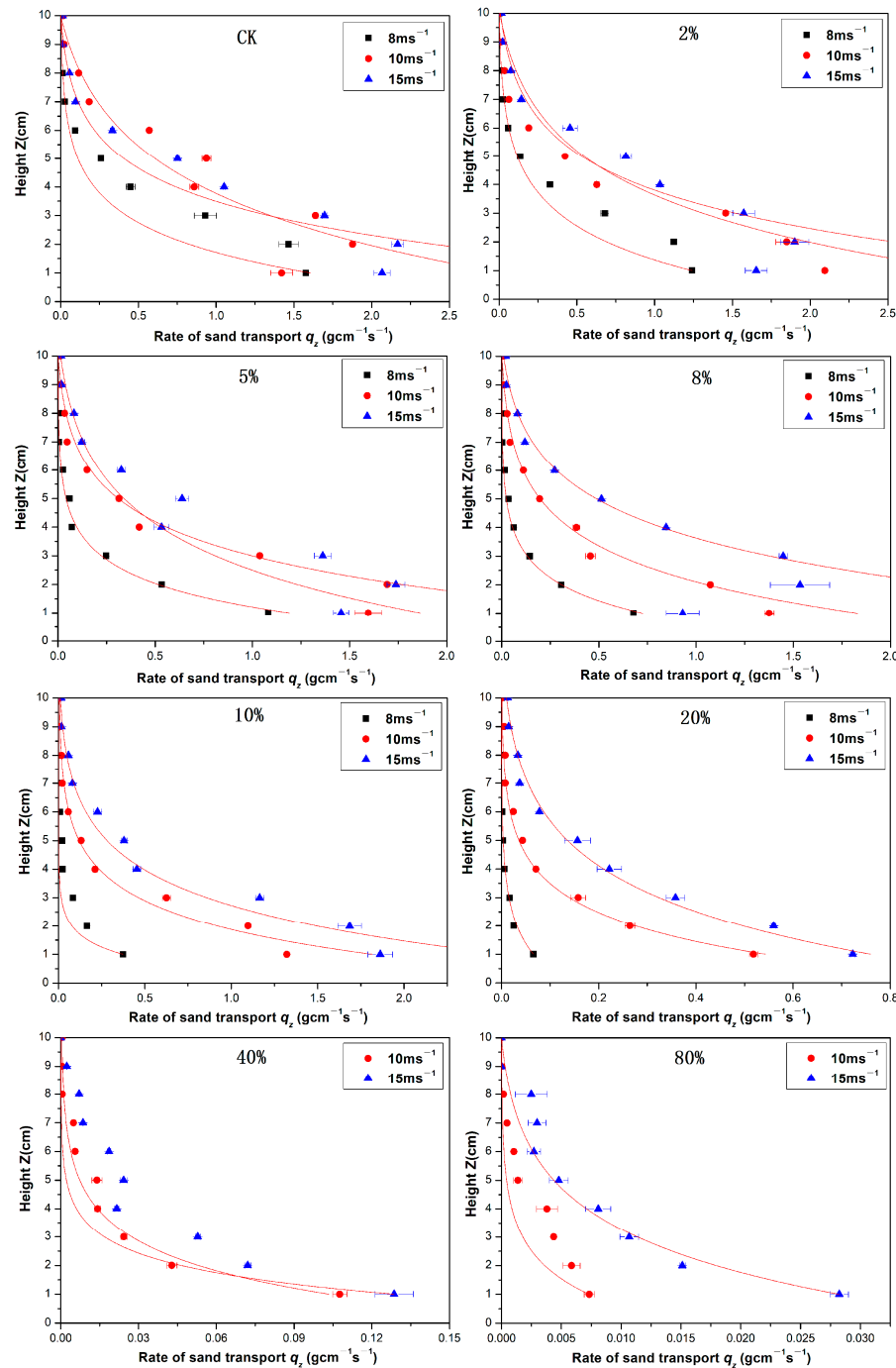


Figure 7. Height variation (Z) in sediment horizontal mass flux changes with various SCB coverages and wind speeds under unsaturated sand flow. The red curves are the sand transport decay curves on the SCB mulch sand bed (Equation (2)). In addition, the sand flux was not observed at 8 ms^{-1} under 40% and 80% SCB coverage.

4. Conclusions

SCBs could be a feasible sand retention material. SCB coverage strongly affected wind erosion efficiency through influencing the interaction between the wind and sand bed under both saturated and unsaturated sand flows. The saturated sand flow process was mainly characterized as deposition, whereas the unsaturated flow process was characterized as aeolian erosion. When the SCB coverage exceeded 40%, the transported sand amount remained constant, and a general balance between erosion and deposition processes was reached, which was stable.

The horizontal mass flux vertical profile decayed exponentially on the SCB mulch sand surface under both saturated and unsaturated sand flow conditions. The horizontal mass flux vertical profile under saturated sand flow resembled the sand surface, with increased curvature near the top layer. The bed characteristics mainly involved transportation and deposition processes. The horizontal mass flux vertical profile under saturated sand flow was similar to that at the sand surface, and the profile curvature increased near the surface. The bed processes were mainly transport and deposition processes. Maximum sand transport occurred at 0–6 cm above the surface due to the increasing interaction between the wind-sand flow and wind-sand bed under low SCB coverage. Vertical particle movement was more responsive to changes at higher SCB coverage levels (10–40%) compared to that at lower SCB coverage levels (below 10%). However, when the SCB coverage exceeded 40%, sand transport still occurred under saturated wind and sand flows, but the bed surface became saturated and wind erosion or accumulation phenomena were not observed on the bed surface. Under unsaturated sand flow, sand transport was essentially impenetrable. The saltating sand particles could reach up to 4 cm or less above the surface, as only the wind momentum was transferred to the SCB particles and saltating sand.

Author Contributions: Conceptualization, J.Z., H.W., and B.H.; methodology, J.Z.; software, H.W.; validation, J.Z., H.W., and B.H.; formal analysis, B.H.; investigation, H.W.; resources, H.W.; data curation, B.H.; writing—original draft preparation, J.Z.; writing—review and editing, J.Z.; visualization, J.Z.; supervision, H.W.; project administration, B.H.; funding acquisition, B.H. All authors have read and agreed to the published version of the manuscript.

Funding: This research was funded by the Third Xinjiang Scientific Expedition Program (grant number 2021xjkk0301) and the Major Science and Technology Projects of Xinjiang Uygur Autonomous Region (grant number 2022A02007-2-1).

Institutional Review Board Statement: Not applicable.

Informed Consent Statement: Not applicable.

Data Availability Statement: Dataset available on request from the authors. The data are not publicly available due to privacy.

Conflicts of Interest: The authors declare no conflicts of interest.

Appendix A

Table A1. Vertical distribution of wind-blown sand flow over SCB mulch beds with different coverages and wind velocities under saturated sand flow.

Coverage	0			5%			10%			20%			40%			80%		
Wind Velocity (ms^{-1})	8	10	15	8	10	15	8	10	15	8	10	15	8	10	15	8	10	15
0–2 cm	10.16	18.31	35.31	9.31	20.62	33.65	7.78	18.88	34.19	7.61	9.98	32.16	7.22	14.11	25.92	7.48	15.23	24.99
2–4 cm	1.94	9.84	19.45	1.38	6.58	19.24	1.42	6.01	16.51	1.28	3.38	16.12	2.05	7.31	16.55	1.72	7.04	13.13
4–6 cm	0.80	4.86	6.89	0.46	2.81	8.14	0.59	2.94	7.86	0.53	1.66	9.55	0.95	3.83	9.42	0.68	3.97	8.99
6–15 cm	0.45	2.52	6.05	0.14	1.81	4.45	0.25	2.17	5.89	0.29	1.13	7.55	0.69	3.96	7.18	0.36	2.52	6.28

Table A2. Vertical distribution of wind-blown sand flow over SCB mulch beds with different coverages and wind velocities under unsaturated sand flow.

Coverage	0			5%			10%			20%			40%			80%		
	Wind Velocity (ms ⁻¹)	8	10	15	8	10	15	8	10	15	8	10	15	8	10	15	8	10
0–2 cm	3.10	8.35	11.13	1.61	6.48	10.66	0.54	4.83	11.50	0.10	1.54	4.25	0	0.30	0.65	0	0.03	0.17
2–4 cm	1.45	5.53	8.36	0.32	2.91	6.51	0.11	1.62	5.29	0.02	0.44	1.92	0	0.08	0.24	0	0.02	0.07
4–6 cm	0.35	2.21	5.07	0.08	0.98	3.34	0.03	0.37	2.01	0	0.14	0.72	0	0.04	0.14	0	0.00	0.02
6–10 cm	0.05	0.36	1.17	0.01	0.23	0.76	0	0.11	0.57	0	0.05	0.33	0	0.01	0.06	0	0.00	0.01

References

- Chepil, W.S.; Woodruff, N.P. The physics of wind erosion and its control. *Adv. Agron.* **1963**, *15*, 211–302. [[CrossRef](#)]
- Overpeck, J.; Anderson, D.; Trumbore, S.; Prell, W. The southwest Indian monsoon over the last 18000 years. *Clim. Dyn.* **1996**, *12*, 213–225. [[CrossRef](#)]
- Schwartz, J. Air pollution and daily mortality: A review and meta-analysis. *Environ. Res.* **1994**, *64*, 36–52. [[CrossRef](#)]
- Akbari, M.; Shalamzari, M.J.; Memarian, H.; Gholami, A. Monitoring desertification processes using ecological indicators and providing management programs in arid regions of Iran. *Ecol. Indic.* **2020**, *111*, 106011. [[CrossRef](#)]
- Li, A.; Zhang, J.; Wang, A. Utilization of starch and clay for the preparation of superabsorbent composite. *Bioresour. Technol.* **2007**, *98*, 327–332. [[CrossRef](#)]
- Abulimiti, M.; Wang, J.; Li, C.; Zhang, Y.; Li, S. Bentonite could be an eco-friendly windbreak and sand-fixing material. *Environ. Technol. Innov.* **2023**, *29*, 102981. [[CrossRef](#)]
- Xin, G.W.; Huang, N.; Zhang, J.; Dun, H.C. Investigations into the design of sand control fence for Gobi buildings. *Aeolian Res.* **2021**, *49*, 100662. [[CrossRef](#)]
- Zang, Y.X.; Gong, W.; Xie, H.; Liu, B.L.; Chen, H.L. Chemical sand stabilization: A review of material, mechanism and problems. *Environ. Technol. Rev.* **2015**, *4*, 119–132. [[CrossRef](#)]
- Fattah, S.M.; Soroush, A.; Huang, N. Wind erosion control using inoculation of aeolian sand with cyanobacteria. *Land. Degrad. Dev.* **2020**, *31*, 2104–2116. [[CrossRef](#)]
- Li, C.J.; Lei, J.Q.; Zhao, Y.; Xu, X.W.; Li, S.Y. Effect of saline water irrigation on soil development and plant growth in the Taklimakan Desert highway shelterbelt. *Soil. Till. Res.* **2015**, *146*, 99–107. [[CrossRef](#)]
- Pi, H.; Huggins, D.R.; Sharratt, B. Wind erosion of soil influenced by clay amendment in the inland Pacific Northwest, USA. *Land. Degrad. Dev.* **2021**, *32*, 241–255. [[CrossRef](#)]
- Nickling, W.G.; Neuman, M.K. Development of deflation lag surfaces. *Sedimentology* **1995**, *42*, 403–414. [[CrossRef](#)]
- Gillette, D.; Goodwin, P.A. Microscale transport of sand-sized soil aggregates eroded by wind. *J. Geophys. Res.* **1974**, *79*, 4080–4084. [[CrossRef](#)]
- Dong, Z.; Liu, X.; Wang, X. Aerodynamic roughness of gravel surfaces. *Geomorphology* **2002**, *43*, 17–31. [[CrossRef](#)]
- Zhang, K.C.; Qu, J.J.; Zu, R.P.; Ta, W.Q. Characteristics of wind blown sand on Gobi and mobile sand surface. *Environ. Geol.* **2008**, *54*, 411–416. [[CrossRef](#)]
- Wang, X.M.; Hua, T.; Zhang, C.X.; Lang, L.L.; Wang, H.T. Aeolian salts in Gobi deserts of the western region of Inner Mongolia: Gone with the dust aerosols. *Atmos. Res.* **2012**, *118*, 1–9. [[CrossRef](#)]
- Zhang, K.; Zhang, W.; Tan, L.; An, Z.; Zhang, H. Effects of gravel mulch on aeolian transport: A field wind tunnel simulation. *J. Arid. Land.* **2015**, *7*, 296–303. [[CrossRef](#)]
- Tan, L.H.; Zhang, W.M.; Qu, J.J.; Zhang, K.C.; An, Z.S.; Wang, X. Aeolian sand transport over gobi with different gravel coverages under limited sand supply: A mobile wind tunnel investigation. *Aeolian Res.* **2013**, *11*, 67–74. [[CrossRef](#)]
- De Vries, S.; de Vries, J.S.M.v.T.; Rijn, L.C.; Arens, S.M.; Ranasinghe, R. Aeolian sediment transport in supply limited situations. *Aeolian Res.* **2014**, *12*, 75–85. [[CrossRef](#)]
- Ren, C.Y.; Wu, S.Z. Effects of Sediment Supply on Aeolian Saltation Transport. *J. Desert Res.* **2011**, *31*, 597–601.
- Wilcock, P.R.; Kenworthy, S.T.; Crowe, J.C. Experimental study of the transport of mixed sand and gravel. *Water Resour. Res.* **2001**, *37*, 3349–3358. [[CrossRef](#)]
- Cai, D.X.; Li, S.Y.; Gao, X.; Lei, J.Q. Wind tunnel simulation of the aeolian erosion on the leeward side of barchan dunes and its implications for the spatial distribution patterns of barchan dunes. *Catena* **2021**, *207*, 105583. [[CrossRef](#)]
- Zhang, W.; Wang, T.; Wang, W.; Wang, T. Wind tunnel experiments on vertical distribution of wind-blown sand flux and change of the quantity of sand erosion and deposition above gravel beds under different sand supplies. *Environ. Earth Sci.* **2011**, *64*, 1031–1038. [[CrossRef](#)]
- Zhang, D.S.; Wu, W.Y.; Tian, L.H.; Wei, D. Effects of Erosion and Deposition and Dimensions Selection of Straw-checkerboard Barriers in the Desert of Qinghai Lake. *Acta Geogr. Sin.* **2014**, *66*, 426–435.
- Liu, L.Y.; Liu, Y.Z.; Li, X.Y. Effect of gravel mulch restraining soil deflation by wind tunnel simulation. *J. Desert Res.* **1999**, *19*, 60–62.

26. Liu, B.L.; Zhang, W.M.; Qu, J.J.; Zhang, K.C.; Han, Q.J. Controlling windblown sand problems by an artificial gravel surface: A case study over the gobi surface of the Mogao Grottoes. *Geomorphology* **2011**, *134*, 461–469. [[CrossRef](#)]
27. Buyantogtokh, B.; Kurosaki, Y.; Tsunekawa, A. Effect of stones on the sand saltation threshold during natural sand and dust storms in a stony desert in Tsogt-Ovoo in the Gobi Desert, Mongolia. *J. Arid. Land.* **2021**, *13*, 653–673. [[CrossRef](#)]
28. Li, H.; Zou, X.; Zhang, C.; Kang, L.; Cheng, H.; Liu, B.; Liu, W.; Fang, Y.; Yang, D.; Wu, X. Effects of gravel cover on the near-surface airflow field and soil wind erosion. *Soil. Till Res.* **2021**, *214*, 105133. [[CrossRef](#)]
29. Nickling, W.G.; Neuman, M.K. Wind tunnel evaluation of a wedge-shaped aeolian sediment trap. *Geomorphology* **1997**, *18*, 333–345. [[CrossRef](#)]
30. Li, X.Y.; Liu, L.Y. Effect of gravel mulch on aeolian dust accumulation in the semiarid region of northwest China. *Soil. Till Res.* **2003**, *70*, 73–81. [[CrossRef](#)]
31. Al-Awadhi, J.M.; Willetts, B.B. Sand transport and deposition within arrays of non-erodible cylindrical elements. *Earth Surf. Process. Landf.* **1999**, *24*, 423–435. [[CrossRef](#)]
32. Xue, X.; Zhang, W.; Wang, T. Wind tunnel experiments on the effects of gravel protection and problems of field surveys. *Acta Geogr. Sin.* **2000**, *55*, 375–383.
33. Zhang, W.; Tao, W.; Xian, X.; Wang, W.; Guo, Y.; Liu, J. The discuss of comprehensively preventing blown-sand system in Mogao Grottoes, Dunhuang. *J. Desert Res.* **2000**, *20*, 409–414.
34. Zhang, W.; Wang, T.; Wang, W.; Qu, J.; Xue, X.; Yao, Z. The Gobi sand stream and its control over the top surface of the Mogao Grottoes, China. *Bull. Eng. Geol. Environ.* **2004**, *63*, 261–269. [[CrossRef](#)]
35. Wang, W.; Dong, Z.; Wang, T.; Zhang, G. The equilibrium gravel coverage of the deflated Gobi above the Mogao Grottoes of Dunhuang, China. *Environ. Geol.* **2006**, *50*, 1077–1083. [[CrossRef](#)]
36. Zheng, X.J.; He, L.H.; Wu, J.J. Vertical profiles of mass flux for windblown sand movement at steady state. *J. Geophys. Res.* **2004**, *109*, B01106. [[CrossRef](#)]
37. Gillette, D.A.; Stockton, P.H. The effect of nonerodible particles on wind erosion of erodible surfaces. *J. Geophys. Res. Atmos.* **1989**, *94*, 12885–12893. [[CrossRef](#)]
38. Wu, Z. *Geomorphology of Blown Sand and Their Controlled Engineering*; Science Press: Beijing, China, 2003; pp. 341–352. (In Chinese)

Disclaimer/Publisher’s Note: The statements, opinions and data contained in all publications are solely those of the individual author(s) and contributor(s) and not of MDPI and/or the editor(s). MDPI and/or the editor(s) disclaim responsibility for any injury to people or property resulting from any ideas, methods, instructions or products referred to in the content.